Relativistic Dynamics: The Relations Among Energy Momentum and Velocity of Electrons and the Measurement of e/m

Mero Elmarassy*
MIT Department of Physics
(Dated: April 9, 2025)

Newtonian mechanics provides an excellent description of the mechanics of almost any object we can think of, from cars to projectiles or even planets. One might think that Newtonian mechanics is all there is to physics, but unfortunately some experiments at higher energies reveal that it does not explain everything. In this experiment we will test the limits of Newtonian mechanics and provide evidence that the theory of special relativity must replace it.

This paper compares the Newtonian and relativistic theories of physics by testing their ability to explain energy, velocity, and momentum relations of relativistic electrons. Measurements of these observables are obtained using a spherical magnet generating a uniform field, a velocity selector, and a PIN Diode. Plots of the Newtonian and relativistic relations are compared to examine their e ectiveness in explaining our observations. Relativistic relations are used to compute $m_e c^2 = 538 \pm 30\text{keV}$, $\frac{e}{m} = (1.66 \pm 0.07) \quad 10^{11} \frac{}{kg}$.

I. RELEVANT THEORY

I.1. Electromagnetism

A particle of charge q and velocity $\vec{v}$ in an electromagnetic field experiences the Lorentz force

$$\vec{F} = q(\vec{E} + \vec{v} \times \vec{B}) \tag{1}$$

where $\vec{E}$ and $\vec{B}$ are the electric and magnetic fields. Due to the Lorentz force, a particle of mass m moving perpendicular to a magnetic field (in the absence of any electric field) follows a circular trajectory with radius

$$r = \frac{p}{q|\vec{B}|} \tag{2}$$

where p is the magnitude of the electron momentum [1]. A uniform electric field applied opposite to $\vec{v} \times \vec{B}$ will exactly oppose the magnetic field when $v = \frac{|\vec{E}|}{|\vec{\ }|}$, but for other speeds the electrons will be deflected. Throughout our experiment, we use a parallel plate velocity selector that relies on this idea to accurately measure velocities of electrons.

I.2. Relativistic Dynamics

According to Newtonian dynamics, the kinetic energy K, momentum $\vec{p}$, and velocity $\vec{v}$ are related by

$$\vec{p} = m\vec{v} \tag{3}$$

$$K = \frac{|\vec{p}|^2}{2m} \tag{4}$$

for a particle of mass m. On the other hand, relativity predicts the relations

$$\vec{p} = \gamma m \vec{v} \tag{5}$$

$$K = (\gamma \quad 1)mc^2 \tag{6}$$

where γ is the Lorentz factor defined by

$$\gamma = \frac{1}{\sqrt{1 \quad \frac{|\vec{v}|^2}{c^2}}} \tag{7}$$

The Newtonian relations emerge as a low-velocity limit of the relativistic ones. Therefore both theories provide accurate predictions at low velocities, but as we will demonstrate, Newtonian physics does not agree with experiment at higher velocities.

II. EXPERIMENTAL SETUP

The experimental setup is shown in Fig 1. The experiment was housed within a spherical magnet producing a uniform vertical magnetic field. A small quantity of ^{9} Sr emitting alpha radiation was used as a source of high energy electrons. The setup was placed in a vacuum chamber held under $10^{\ \ 4}$ Torr to minimize distortion due to scattering of electrons. Placed on the other side of the sphere was a parallel plate velocity selector used to filter the velocities of incoming electrons. Incoming electrons were detected by a PIN diode at the end of the selector, and fed to a multi channel analyzer (MCA) used to bin the count data.

The magnetic field values were measured with a gaussmeter to a precision of roughly 1%. Additionally, measurements of the magnetic field were taken at ten points along the electron trajectories and were found to vary less than 1%. Therefore throughout the rest of the paper we assume the field is uniform and take a systematic error of 1% on our magnetic field measurements.

* mero@mit edu

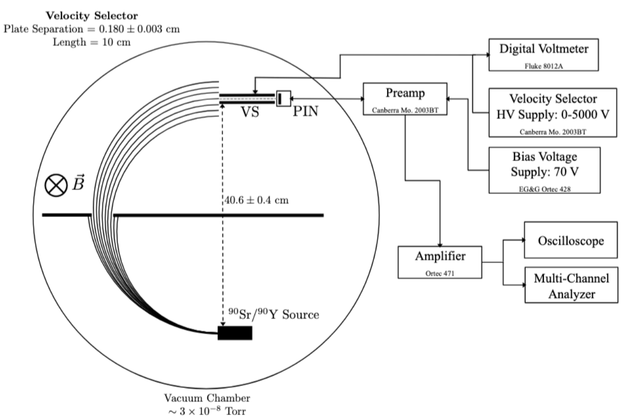

FIG. 1. Schematic diagram of the electron trajectory in the apparatus, spectrometer, and associated circuitry. The velocity selector is labeled VS and the diode detector PIN. Image from [1].

III. EXPERIMENTAL PROCEDURE

III.1. Calibration

We calibrated the MCA channels to their corresponding energies using a sample of ^{133}Ba, which has a known spectrum with several distinctive peaks spread across the range of the MCA. A main calibration session, lasting roughly two days, was run at the start of the experiment (results shown in Fig 2). Additionally, short sessions lasting roughly 15 minutes were run at the start of each data taking day to ensure the calibration stayed consistent across days. Finally, we used magnets of known field strength to calibrate the gaussmeter each day of data taking.

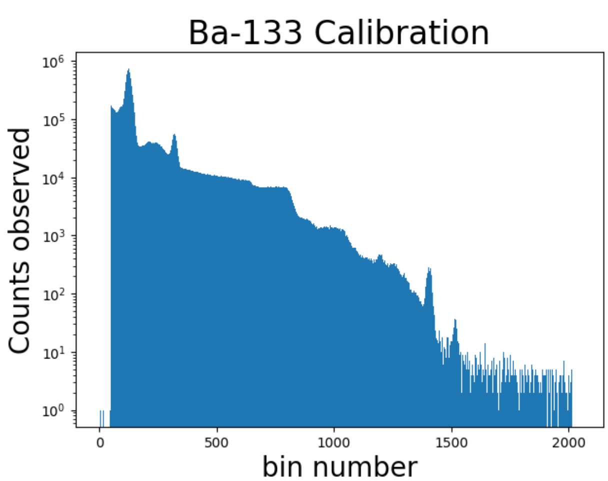

FIG. 2. Plot of two-day Ba-133 Calibration (log scale). Characteristic peaks in spectrum of Ba-133, such as 30.97kV, 81.00kV, and 302.90kV, are clearly identifiable.

III.2. Data taking

We took data at five values of B ranging from 70 to 120. For each field, we took energy spectra at several di erent voltages. We fit a gaussian to each spectrum, allowing us to obtain a mean and uncertainty on the peak channel number. We took the number of counts to be the integral of the fit gaussian, and computed the count rate by dividing by the live time of the detector. Due to the negligible time uncertainties, we took the count rate uncertainty to be the Poissonian uncertainty of the counts divided by the live time.

We took step sizes of $0.05kV$ - $0.1kV$ to roughly map the shape of the rate to voltage curve. Once the general location of the peak count rate was determined, we did finer step sizes near the peak. We used this to precisely identify V , the voltage that maximizes the count rate.

Finally, throughout the experiment we periodically monitored the gauge on the vacuum chamber to ensure it was below 10 ^{4} Torr. This ensured that scattering of electrons due to gas in the chamber would be negligible.

IV. DATA ANALYSIS

IV.1. Calibration: Fitting MCA Channels to Kinetic Energies

To obtain a mapping of MCA channels to kinetic energies, we identified the known peaks in the spectrum of the Ba-133 calibration data shown in Fig 2. We estimated the uncertainty in the channel number of each peak as the number of channels in its width. Due to the fact that MCA data is linear, we performed a linear fit on this mapping of channel numbers to energies to obtain a full mapping for each channel of the MCA. The results of the fit are summarized in Fig 3. The uncertainties in the kinetic energies were estimated as the uncertainty in a, the slope fit parameter of the line.

IV.2. Energy Spectra

As discussed earlier, we took energy spectra measurements for several voltages at each field. Using our calibration fit above, we mapped the MCA channels onto energies and fit a gaussian to each spectrum, as shown in Fig 4. The gaussian fits were integrated to obtain the total counts for each spectrum. The mean and standard deviations were used as estimates for the value and uncertainty of the kinetic energy for each spectrum.

IV.3. Finding V

To find the peak voltage V that maximizes the count rate for each field, we performed fits to the count rates

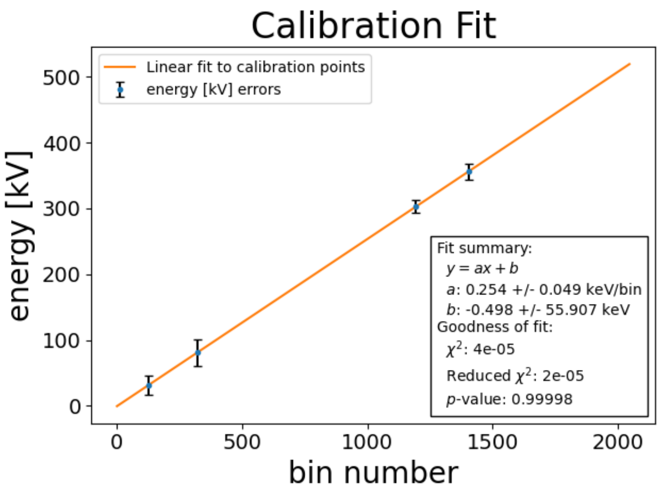

FIG. 3. Linear fit to energies as a function of MCA channel number.

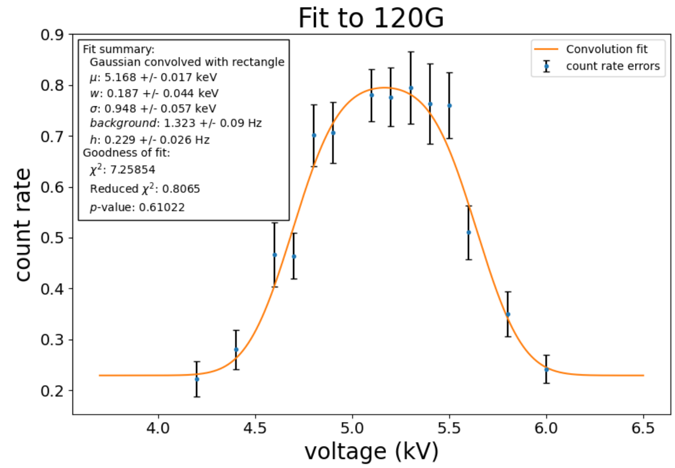

FIG. 5. Fit of rectangle convolved with gaussian to 120G field data.

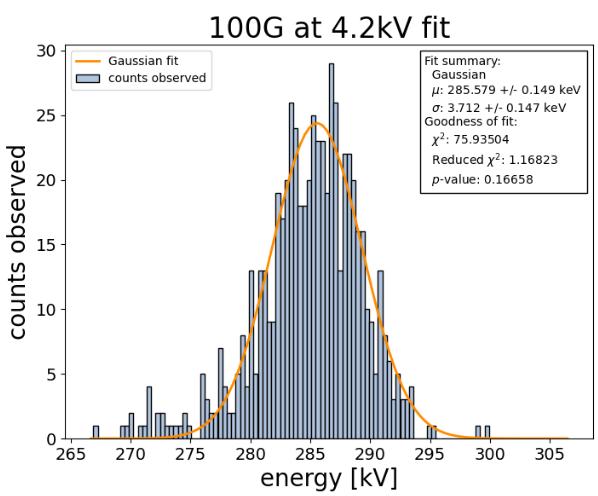

FIG. 4. Gaussian fit to the energy spectrum at 100G and 4.20kV.

obtained from our energy spectra. For each field value, we plotted count rate as a function of voltage. Since the nonzero width of the velocity selector provides some margin for error on the peak voltage, we decided to fit to a rectangle convolved with a gaussian. The rectangle accounts for the flat range of possible V values, and the gaussian convolution smoothens out the curve. This functional form was mostly obtained empirically by analyzing the shape of the distributions, but it provided good agreement with our data, as shown in Fig 5.

We took our peak voltage to be the mean value of the gaussian, and our uncertainty was the half width of the rectangle.

IV.4. Relativistic t: determining rest energy m_ec^2

Recall from equation (6) that relativity predicts a linear relationship between $\gamma \quad 1$ and K, with a slope equal to the rest energy of the electron, m_ec^2. Here we have $\gamma = \overline{1 \quad {}^2}$, where $= \frac{E}{c}$ and $E = V/d$ is the electric field. The errors in γ are computed by propagating the V and B errors. The γ errors were roughly on the same order as the K errors, so an orthogonal least-squares fit was done to the data [2]. The results are shown in Fig 5, and we obtained $m_ec^2 = 538 \pm 30$keV.

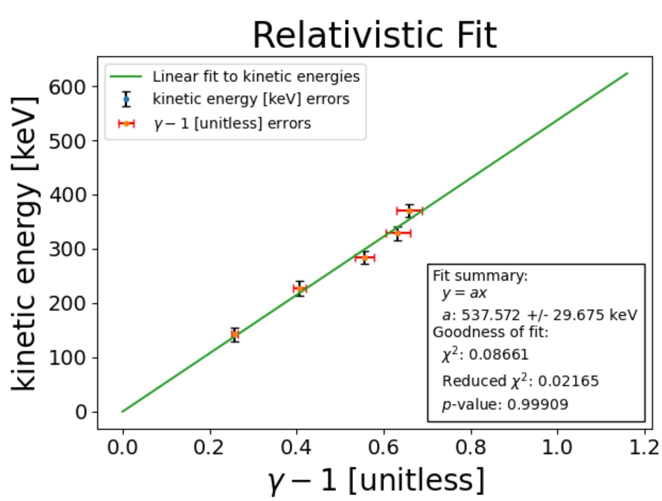

FIG. 6. Fit of relativistic kinetic energy-velocity relation. Slope gives electron rest energy as 538 ± 30keV.

IV.5. Determining electron charge to mass ratio $\frac{e}{m}$

Combining (2) with the relativistic energy and momentum formulas yields

$$B = \frac{c/r}{e/m}\ \gamma \tag{8}$$

Thus, fitting the magnetic field values linearly against γ, we can obtain the electron charge to mass ratio $\frac{e}{m}$ as $\frac{c}{ra}$ where a is the slope of the fit line.

As in IV.4, the uncertainties in γ are computed by propagating the uncertainties in E and B. Since the γ errors were not negligible compared to the B errors, we followed the techniques of Bevington to compute the adjusted errors [3]. We then performed a linear fit, summarized in Fig 7. From our slope we computed a final value of $\frac{e}{m} = (1.66 \pm 0.07) \times 10^{11} \frac{C}{kg}$, which is in good agreement with the known value of $1.76 \times 10^{11} \frac{C}{kg}$

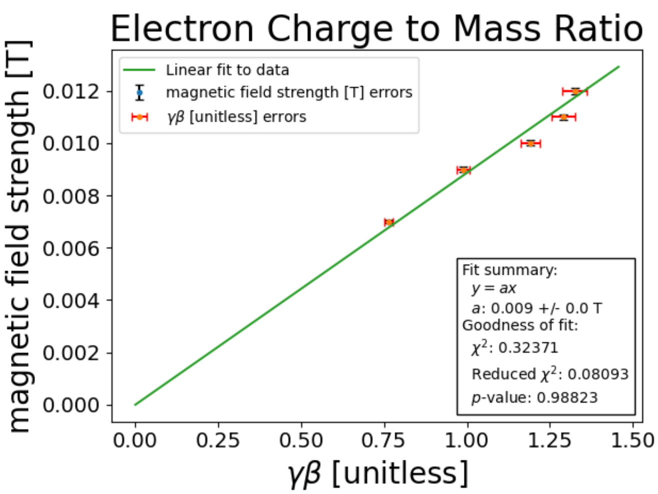

FIG. 7. Linear fit of magnetic field values to γ values. Slope a gives electron charge-mass ratio through $\frac{e}{m} = \frac{c}{ra}$.

IV.6. Newtonian Fit

As is readily seen from equations (3) and (4), Newtonian mechanics predicts $K = \frac{1}{2}mv^2$. We then use $v = c\frac{E}{\ }$ to obtain $K = \frac{m\ c^2}{2}\frac{E^2}{\ ^2}$. Therefore if Newtonian mechanics accurately models our observations, a quadratic fit to these data points should yield the electron rest energy.

However, fitting with the function $\frac{m\ c^2}{2}x^2$ (shown in Fig 8) yields $m_ec^2 = 1027 \pm 20$keV, more than 20 standard deviations away from the known value of 514keV. Thus it is extremely unlikely that classical mechanics explains our observations.

On the other hand, plotting the relativistic energy-velocity relation with our previously found electron rest energy from IV.4 yields a far better agreement (Fig 8).

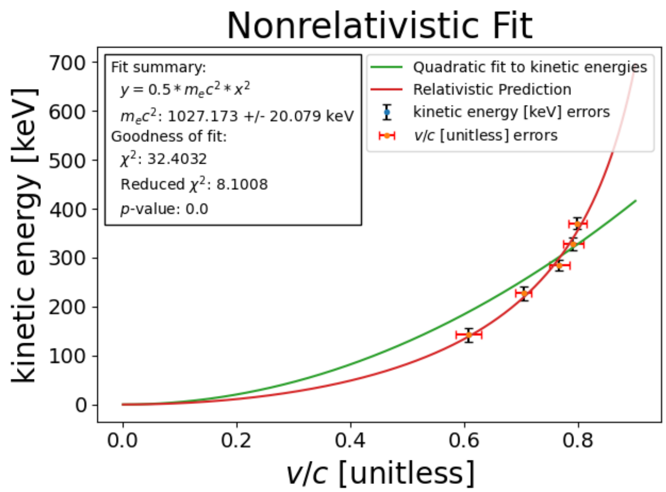

FIG. 8. Classical energy-velocity relation fit to data, with poor results. Relativistic energy-velocity relation shows far better agreement.

IV.7. Determining electron charge e

Using our values for $\frac{e}{m}$ and m_ec^2, and propagating the errors into $e = \frac{1}{c^2}\frac{e}{m}m_ec^2$, we obtain $e = (1.59 \pm 0.11) \times 10^{\ 19}$C, which agrees well with the known value of $1.602 \times 10^{\ 19}$C.

V. CONCLUSIONS

Our relativistic results for the electron rest energy $m_ec^2 = 538 \pm 30$keV and the electron charge-mass ratio $\frac{e}{m} = (1.66 \pm 0.07) \times 10^{11} \frac{C}{kg}$ both agree with their true values within uncertainty. Additionally, the relativistic fit results all converged with low reduced χ^2 values, indicating that they were good fits to our observations. In contrast, the non-relativistic fit did not converge to our data and gave us an electron rest energy more than twenty standard deviations away from the true value. Thus, we can conclude that the relativistic theory provides a better explanation for our results as compared to the Newtonian theory, reaffirming that Newtonian mechanics is not valid for high speeds.

ACKNOWLEDGMENTS

Mero Elmarassy gratefully acknowledges Maryna Bohdan for her help with this experiment.

[1] M. D. of Physics, *8 13 Relativistic Dynamics Lab Guide*, MIT (2024).

[2] "Orthogonal regression," .

[3] P. Bevington and D. Robinson, *Data Reduction and Error Analysis for the Physical Sciences* (McGraw-Hill, 2003).